ACS APPLIED MATERIALS & INTERFACES

Research Article

www.acsami.org

Amphiphilic Polymer-Mediated Formation of Laponite-Based Nanohybrids with Robust Stability and pH Sensitivity for Anticancer Drug Delivery

Guoying Wang,[†,‡] Dina Maciel,[†,‡] Yilun Wu,[⊥] João Rodrigues,[‡] Xiangyang Shi,[‡,⊥] Yuan Yuan,[§] Changsheng Liu,[§] Helena Tomás,*[,‡] and Yulin Li*[,‡,§]

[‡]CQM—Centro de Química da Madeira, MMRG, Universidade da Madeira, Campus Universitário da Penteada, 9020-105 Funchal, Portugal

[§]The State Key Laboratory of Bioreactor Engineering and Key Laboratory for Ultrafine Materials of Ministry of Education, East China University of Science and Technology, Shanghai 200237, People's Republic of China

[⊥]College of Chemistry, Chemical Engineering and Biotechnology, Donghua University, Shanghai 201620, People's Republic of China

Supporting Information

ABSTRACT: The development of pH-sensitive drug delivery nanosystems that present a low drug release at the physiological pH and are able to increase the extent of the release at a lower pH value (like those existent in the interstitial space of solid tumors (pH 6.5) and in the intracellular endolysosomal compartments (pH 5.0)) is very important for an efficient and safe cancer therapy. Laponite (LP) is a synthetic silicate nanoparticle with a nanodisk structure (25 nm in diameter and 0.92 nm in thickness) and negative-charged surface, which can be used for the encapsulation of doxorubicin (DOX, a cationic drug) through electrostatic interactions and exhibit good pH sensitivity in drug delivery. However, the colloidal instability of LP still limits its potential clinical applications. In this study, we demonstrate an elegant strategy to develop stable Laponite-based nanohybrids through the functionalization of its surface with an amphiphile PEG—PLA copolymer by a self-assembly process. The hydrophobic block of PEG—PLA acts as an anchor that binds to the surface of drug-loaded LP nanodisks, maintaining the core structure, whereas the hydrophilic PEG part serves as a protective stealth shell that improves the whole stability of the nanohybrids under physiological conditions. The resulting nanocarriers can effectively load the DOX drug (the encapsulation efficiency is 85%), and display a pH-enhanced drug release behavior in a sustained way. In vitro biological evaluation indicated that the DOX-loaded nanocarriers can be effectively internalized by CAL-72 cells (an osteosarcoma cell line), and exhibit a remarkable higher anticancer cytotoxicity than free DOX. The merits of Laponite/PEG—PLA nanohybrids, such as good cytocompatibility, excellent physiological stability, sustained pH-responsive release properties, and improved anticancer activity, make them a promising platform for the delivery of other therapeutic agents beyond DOX.

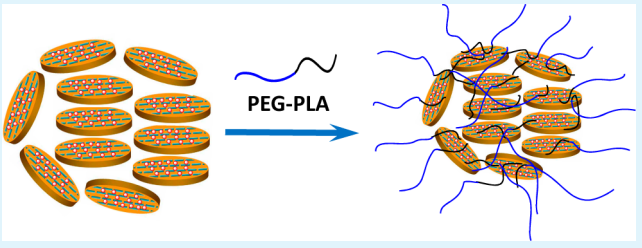

KEYWORDS: *amphiphilic polymer, Laponite, doxorubicin, pH sensitive, anticancer*

INTRODUCTION

Nowadays, cancer is a major healthcare problem around the world.[1] Among anticancer drugs, doxorubicin (DOX) has been widely used for the treatment of various types of cancers. DOX can intercalate the adjacent base pairs of the DNA double helix, and bind DNA-associated enzymes such as topoisomerase enzymes I and II, which block DNA replication and RNA transcription. On the other hand, DOX can itself generate free radicals with high reactivity to induce cytotoxicity on cancer cells.[2] However, its clinical application is still limited by its low efficacy, mainly associated with an ineffective drug influx, increased drug efflux, DNA repair activation, alterability in drug metabolism, detoxification, etc., which is commonly known by drug resistance.[3−7] Therefore, to maintain the needed DOX concentration level, a large dosage or an increased number of injections are often used, which may lead to adverse side effects in normal tissues, especially the heart and the kidneys.[8,9] For this reason, various nanosystems, including dendrimers,[10] liposomes,[11] micelles,[12] inorganic nanoparticles,[13,14] and nanogels,[15] have been explored for administration of DOX.[16] The ideal nanocarrier can maintain a limited drug release during circulation, achieve an enhanced accumulation in the tumor tissue, penetrate cells easily and release the drug inside tumor cells in a controlled manner, thus resulting in an improved efficacy and decreased side effects by reducing the amount of drug needed.[17] However, few nanocarriers are effectively able to

Received: June 10, 2014
Accepted: August 28, 2014
Published: August 28, 2014

handle the drug resistance-associated problems (for instance, due to their poor cell uptake ability, insufficient intracellular delivery capacity, etc.), and/or present a sufficient physiological stability.[3]

Among nanomaterials, nanoclays are emerging as a new potential candidate for biomedical applications, because of their biocompatibility, bioactive interface, and controlled drug release properties.[18] Laponite (LP) is a synthetic nanoclay that has a nanodisk structure (25 nm in diameter and 0.92 nm in thickness), and can be biodegraded into nontoxic products (Na^+, $Si(OH)_4$, Mg^{2+}, Li^+), very much similar to what happens with bioactive glasses (Na^+, $Si(OH)_4$, Ca^{2+}, PO_4^{3-}).[19] The chemical structure of the LP crystals confer them a negatively charged surface and pH-dependent edge surface charges (positive at a pH lower than 9).[19] Its unique structure, together with its good biocompatibility,[20] and osteoinductivity,[21] makes LP act as an ideal inorganic nanomaterial for biomedical applications.[22] However, few studies have been made using it as a nanoplatform for drug delivery.[23] Previously, our group prepared LP reinforced alginate bulk hydrogels, which showed a significant increase in the loading capacity of DOX, and enhanced drug release sustainability and anticancer cytotoxicity.[7] Furthermore, other studies revealed that, through electrostatic interactions, DOX was able to form nanocomplexes with LP, which improved the bioactivity of the drug in cancer cells by overcoming drug resistance processes.[24] Unfortunately, even though they assume a nanoscaled size in water, the nanocomplexes tend to aggregate under physiological conditions, probably because the existence of various ionic compounds changes the dispersed state of LP.[24]

Since LP has an ability to form strong interactions with hydrophobic molecules,[25,26] it is proposed that an amphiphilic block polymer can be used to form a protective coating on LP nanodisks, where the hydrophobic block will cover the surface of LP nanodisks working as an anchor, whereas the hydrophilic part will act as a stealth shell to maintain their stability under physiological environment. Herein, we present an elegant approach to preparing a new type of pH-sensitive LP-based nanocarriers with good cytocompatibility and stability, which are able to sustain the DOX release in an acidic-accelerated mode, and achieve an improved anticancer activity.

MATERIAL AND METHODS

Materials. Laponite RDS (LP) was friendly offered from Rockwood Additives Limited, UK. Poly(ethylene glycol)−poly(lactic acid) diblock copolymer (PEG−PLA, with molecular weight 8000 Da), which was composed of a 50:30 weight ratio of ethylene glycol and lactic acid units, was purchased from Jinan Daigang Biological Technology Co, Ltd., China. Poly(ethylene glycol) (PEG, with molecular weight 6000 Da) was purchased from Sigma-Aldrich, UK. Doxorubicin hydrochloride (DOX) was obtained from Zibo Ocean International Trade Co, Ltd., China. Dulbecco's phosphate buffer saline (PBS, without Ca^{2+} and Mg^{2+}) solution was bought from Sigma. All other reagents were from Sigma, unless otherwise indicated.

Preparation and Characterization of LP/DOX/PEG−PLA Nanohybrids (LDP). LP was dispersed in ultrapure (UP) water under sonication (BRANSON 2510, 100 W) for 30 min to obtain solutions with different LP concentrations (4, 5, 6, and 7 mg/mL). Two mg/mL DOX aqueous solution was prepared using the similar procedure. After that, LP and DOX solutions (2:1 by volume ratio) were mixed under magnetic stirring for 24 h to allow for the thorough interaction of DOX with LP to produce LP/DOX nanocomplexes. The PEG−PLA was dissolved into water/ethanol solution (1:1 by volume) with the concentration 6 mg/mL. Then, the solution of LP/DOX was dropped into the PEG−PLA solution using a weight ratio of LP to PEG−PLA of 1:3, and the mixture underwent magnetic stirring for 5 min. The ethanol was removed by rotatory vacuum evaporation at 40 °C to obtain LP/DOX/PEG−PLA nanohybrids. The free DOX and PEG−PLA were removed from the solutions of LP/DOX nanocomplexes and LP/DOX/PEG−PLA nanohybrids by dialysis against UP water, for 12 h (the dialysis membrane had a molecular weight cutoff of 10 000 Da, Spectrum Laboratories, Inc.), to obtain the final products named as LD and LDP nanohybrids, respectively. The DOX content in the dialysis medium was determined by measuring the DOX fluorescence (λ_{ex} = 480 nm, λ_{em} = 580 nm) using a microplate reader (model Victor^3 1420, PerkinElmer) for calculation of DOX encapsulation efficiency.

Fourier transform infrared (FTIR) spectroscopy was performed using a FTIR spectrometer (PerkinElmer Spectrum Two). All spectra were recorded using a transmission mode with a wavenumber range of 500−4000 cm^{-1}. Ultraviolet−visible (UV−vis) spectroscopy was performed using a Lambda 25 UV−vis spectrometer (PerkinElmer 25). Free DOX, and DOX-loaded nanohybrids were dispersed in water at a DOX concentration of 0.05 mg/mL before measurements. LP and PEG−PLA solutions with concentration of 0.30 and 0.90 mg/mL were also tested as controls.

The hydrodynamic diameter and the surface charge of LP, LD and LDP nanohybrids in water or PBS solution were measured at room temperature using a Zetasizer Nano ZS (Malvern Instruments, UK). The hydrodynamic diameters were determined with a detection angle of 173°. Zeta potential measurements were performed with a detection angle of 17° and calculated using the Smoluchowsky model for aqueous suspensions. Before measurement, LD and LDP nanohybrids were dispersed in UP water or PBS and sonicated (BRANSON 2510, 100 W) for 15 min. To confirm the in vitro physiological stability of the nanohybrids, the sizes of the solution of LD and LDP nanohybrids in water and PBS solution were tracked by the Zetasizer at a specific time interval. The photos of the solutions of LP and LDP in PBS or fetal bovine serum (FBS) buffer at 5 min, 1 and 24 h were taken for direct visualization of their dispersed state.

The morphology of the LP, LD and LDP was examined on a transmission electron microscope (TEM) (JEOL JEM-200CX). Before measurement, the samples were dispersed in UP water under sonication for 15 min. Aqueous suspensions of the samples (0.1 mg/mL) were dropped onto a 100-mesh Formvarcoated copper grid and then air-dried before imaging.

In Vitro Drug Release Studies. The PBS solutions of LD and LDP containing equivalent DOX concentrations (100 μg DOX in 5 mL PBS) were put into a dialysis membrane (molecular weight cutoff of 14, 000 Da), which was placed into 15 mL PBS solution under 100 rpm stirring in an incubator (Unimax 1010, Heidolph) at 37 °C. Different pH values (7.4, 6.5, 5.0) were tested. At a specific time interval, 100 μL of released medium was taken out from each vial, and refreshed with another 100 μL of PBS solution. The released DOX was quantified by measuring the DOX fluorescence using the method mentioned above. The cumulative release (C_r) of DOX against time was obtained according to the equation

$$C_r = 100W_t/W_{tot} \quad (1)$$

where W_t and W_{tot} are the cumulative amount of drug released at time t, and the total drug contained in the nanohybrids used for drug release, respectively.

Biological Assays. CAL-72 cells (an osteosarcoma cell line) and NIH 3T3 fibroblasts cells (a noncancerogenic cell line) were cultured in Dulbecco's Modified Eagle Medium (D-MEM) containing 10% (v/v) fetal bovine serum (FBS, Gibco) and 1% (v/v) of an antibiotic-antimycotic 100x solution (AA, Gibco, with penicillin, streptomycin, and amphotericin B). For CAL-72 cells the medium was also supplemented with 1% (v/v) of L-glutamine 100× solution (Gibco) and 1% (v/v) of insulin-transferin-selenium 100x solution (ITS, Gibco). Cells were grown at 37 °C, in a humidified atmosphere with 5% of carbon dioxide. Afterward, the cells were harvested at 70−80% confluence, using a trypsin-EDTA solution.

To prove if the LD and LDP nanohybrids were therapeutically active, CAL-72 cells and NIH 3T3 fibroblasts cells were first plated in

48-well plates for 24 h, with a seeding density of 10×10^3 cells per well. After 24 h, free DOX, LD and LDP nanohybrid solutions (with equivalent DOX concentrations) were prepared in UP water, added to the cell cultures, and then incubated for 48 h at 37 °C, before performing the resazurin reduction assay to check cell viability. Note that LP and PEG−PLA were used as a control at equivalent mass concentrations to those used for LD and LDP.

The cell viability was quantified by the measurement of the metabolic activity of the cells in culture through the resazurin reduction assay. Briefly, after the 48 h incubation time, the cell culture medium was replaced with fresh medium containing resazurin at a concentration of 0.1 mg/mL and kept at 37 °C in the cell incubator for 3 h. Afterward, aliquots of the cell supernatant were transferred to 96-well opaque plates and the resorufin fluorescence (λ_{ex} = 530 nm, λ_{em} = 590 nm) was measured using a microplate reader (model Victor^3 1420, PerkinElmer). Cell morphology (optical microscopy) and fluorescence microscope images of CAL-72 cells after 48 h culture with free DOX, LD, LDP were also captured by optical fluorescence microscopy (Nikon Eclipse TE 2000E inverted microscope).

For the cell uptake study, CAL-72 cells were plated for 24 h with a density of 20×10^3 cells per well, before incubation with freshly prepared aqueous solutions of DOX, LD or LDP nanohybrids with an equivalent DOX concentration (2.5 μM) at 37 °C for 2 h. Subsequently, the cells were stained with 4′,6-diamidino-2-phenylindole (DAPI, Sigma) for 30 min and fixed with 3.7% (v/v) formaldehyde solution. The cells were then washed with PBS solution for further analysis by optical fluorescence microscopy (Nikon Eclipse TE 2000E inverted microscope). The cell images were analyzed using ImageJ software (open source).

Statistical Analysis. One way ANOVA statistical analysis was performed to compare the cytotoxicity of cells cultured onto different materials using the software Origin 8.0. The p value of 0.05 was selected as the significance level, and the data were indicated with (**) for $p < 0.01$. Each experiment was done in triplicate ($n = 3$). The size statistic of TEM was performed by the software Nano measure.

RESULTS AND DISCUSSION

Preparation and Physical Characterization of Dox-Loaded LP and LDP Nanohybrids. For therapeutic delivery, the size of a nanoplatform plays an important role on its biodistribution. It has been reported that nanoparticles with a size around 100 nm are more able to permeate the immature malignant neovasculature and accumulate in the tumor site through the enhanced permeation and retention (EPR) effect while their uptake by the reticuloendothelial system (RES) occurs in a slower rate.[27−29] As the first step to prepare the nanohybrids involved the electrostatic interaction between DOX and LP,[20,24] we started to optimize the hydrodynamic size of the formed nanocomplexes via dynamic light scattering (DLS), by varying the weight ratio between LP and DOX (as shown in Table 1). We observed that LP alone was dispersed in aqueous solution as individual nanodisks (31 ± 4 nm), but that a decrease of the LP/DOX ratio led to a rapid increase in the size of the formed LP/DOX complexes.[30,31] We found that LP/DOX ratios higher than 6:1 presented a hydrodynamic diameter (98 ± 7 nm) adequate for preparation of the nanohybrids. Therefore, we chose an LP/DOX ratio of 6:1 to prepare the aimed nanohybrids for further experiments.

Table 1. Hydrodynamic Size of LP and LP/DOX Complexes with Different LP/DOX Weight Ratios in Aqueous Solution (DOX Concentration was Fixed at 2 mg/mL)

sample name	LP/DOX (wt:wt)	size (nm)
LD_4:1	4:1	1270 ± 99
LD_5:1	5:1	169 ± 3
LD_6:1	6:1	98 ± 7
LD_7:1	7:1	74 ± 3
LP		31 ± 4

Because of its good biocompatibility and biodegradability, poly(ethylene glycol)−poly(lactic acid) diblock copolymer (PEG−PLA) was employed as a model of an amphiphilic polymer in this study.[32] Therefore, the preparation of the DOX-loaded nanohybrids involved two steps according to the procedure depicted in Scheme 1. First, the cationic DOX drug was mixed with a LP aqueous solution where LP was present as individual nanodisks, to form DOX-loaded LP nanocomplexes (a LP/DOX weight ratio of 6:1 was used as explained before) with high encapsulation efficiency (97.6 ± 0.1%) via electrostatic interactions (Table 2). For simplification, the LP/DOX nanocomplexes will be abbreviated as LD nanocomplexes in the following text. After that, the aqueous solution of LD nanocomplexes was added to PEG−PLA in water/ethanol solution to introduce the PEG−PLA protective layer on the LP surface (ethanol helps to dissolve the hydrophobic PLA block of the PEG−PLA copolymer at the molecular level). Then, ethanol was rapidly removed by rotary evaporation to allow the fixation of PLA segmental chains on the surface of LD nanocomplexes to produce LP/DOX/PEG−PLA nanohybrids (LDP nanohybrids).

Table 2 shows the hydrodynamic diameter (size) of the nanohybrids analyzed by dynamic light scattering (DLS) and the corresponding ζ-potentials. The Z-average size of LP was 31 ± 4 nm, indicating it is well dispersed state in water as individual nanodisks.[21] The addition of DOX resulted in the successful formation of nanocomplexes of LP/DOX (98 ± 7 nm), probably through their strong electrostatic interactions.[20] The incorporation of PEG−PLA appeared to further increase the hydrodynamic size of LP/DOX, indicating the successful coating of the nanocomplexes, which was further confirmed by the less negative ζ-potential of LP/DOX/PEG−PLA (−20.6 ± 3.1 mV) when compared to that of LP/DOX (−37.5 ± 4.5 mV).

The LD and LDP nanocarriers were further characterized by UV−vis and FTIR spectroscopy, with the spectra shown in Figure 1 and 2, respectively. From their UV−vis spectra (Figure 1), we can see that, for the free DOX, LD and LDP nanohybrids, there is an absorption peak at around 480 nm, which is absent in LP and PEG−PLA spectra, indicating the successful loading of DOX in the nanohybrids.[20] As shown in Figure 2, the FTIR spectrum of free DOX presents its own characteristic bands at 1712 (band of C−O), 1582 (bending of NH_2 on aromatic ring), 1412 (bending of NH_2 on aromatic ring), and 1285 cm^{-1} (C−N stretching vibration).[33,34] The peaks located at 1012 and 3448 cm^{-1} in the spectrum of LP, LD, and LDP can be attributed to the −Si−O− stretching vibration and the −OH bending vibration in the LP nanodisks.[35] Compared to pure LP, the LD and LDP nanohybrids present distinctive bands at 1582, 1412, and 1285 cm^{-1} associated with DOX, again indicating that DOX was efficiently encapsulated in the corresponding nanocarriers. Different from LD, LDP gave new bands located at 2889 and 1757 cm^{-1}, which are characteristic of PEG−PLA,[36] demonstrating that PEG−PLA was successfully wrapped on the surface of LP/DOX nanocomplexes.

The morphology and size distribution of the nanoparticles were further characterized by transmission electron microscopy (TEM) imaging (Figure 3). LP, LD, and LDP had average sizes of 51 ± 6, 72 ± 4, and 82 ± 4 nm, respectively (Figure 3). An

Scheme 1. Schematic Representation of Fabrication of LP/DOX (LD nanocomplexes) and LP/DOX/PEG−PLA (LDP nanohybrids) Nanocarriers and Their Stability in PBS Solution

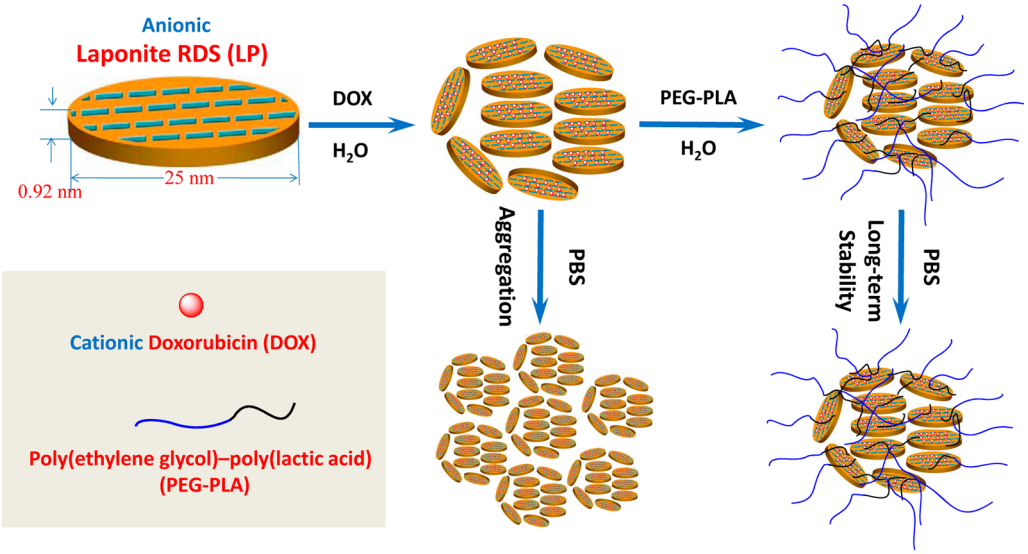

Table 2. Characterization of DOX-Loaded LP and LDP Nanohybrids in Water

sample identity	size (nm)	zeta potential (mV)	EE (%)[a]
LP	31 ± 4	−43.2 ± 3.7	
PEG−PLA	37 ± 1	−8.4 ± 0.8	
LD	98 ± 7	−37.5 ± 4.5	97.6 ± 0.1
LDP	107 ± 5	−20.6 ± 3.1	85.2 ± 4.2

[a]Encapsulation efficiency (EE) = $100W_e/W_0$, W_0 and W_e are the total DOX weight used for loading and the weight of encapsulated DOX, respectively.

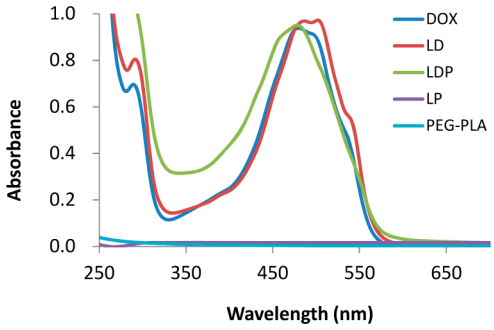

Figure 1. UV−vis spectra of DOX, LP, PEG−PLA, and nanohybrids of LD as well as LDP. Both LD and LDP nanohybrids show a DOX absorption peak at around 480 nm, indicating that DOX was successfully loaded into the nanohybrids.

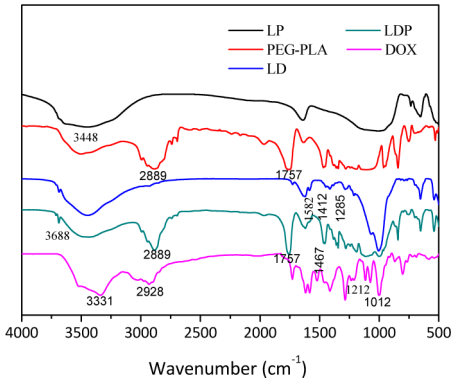

Figure 2. FTIR spectra of DOX, LP, and PEG−PLA and of LD and LDP nanocarriers. The distinctive bands of DOX (1582, 1412, and 1285 cm^{-1}) are also found in the LD and LDP nanohybrids, suggesting a successful DOX loading.

obvious outer layer (lighter shell/darker core) was found on the surface of LDP which, together with its larger size compared to LD, again confirmed the successful coating by PEG−PLA on LD to obtain LDP nanohybrids (Figure 3c). LDP had a slightly less DOX encapsulation efficiency (85.2 ± 4.2%) than LD (97.6 ± 0.1%), which may be caused by the replacement of DOX on LP surface by PEG−PLA after its coating. The LDP nanohybrids thus consisted of: an LP-inner core that serves as a temporarily drug reservoir and affords pH sensitivity in the release of DOX; an outer layer of hydrophilic PEG chains that prevents nanohybrid aggregation under physiological conditions through steric hindrance.[37] It has to be mentioned that because TEM measures the size of the samples in the dry state, the dry process may cause some aggregation of the nanoparticles.

The colloid stability of nanoparticles as a function of time can be evaluated by their hydrodynamic diameter change in physiological conditions. Therefore, the size of the nanoparticles was further monitored by DLS in phosphate buffer saline (PBS) solution and shown in Figure 4. It is can be seen that, even though LD particles had a nanosize in water, they were not stable and quickly formed microsized aggregates.[20] As expected, LDP nanohybrids were able to maintain their long-term stability during the studied period (21 days), which is a very important factor to decide if they can be used in vivo.[38−40] Indeed, in water, PBS solution, or fetal bovine serum (FBS), LDP exhibited an excellent stability when compared with that of LD (Figure 4a−c). As a control, LP was studied in combination with PEG (LD/PEG nanocomplexes, PEG molecular weight of 6000 Da), resulting in the formation of aggregates (353 ± 11 nm in water and 1822 ± 131 nm in PBS solution). Therefore, the stability of LDP should be attributed to a cooperative effect of both PLA and PEG. Because of its hydrophobicity, the segmental chains of PLA adsorb onto the

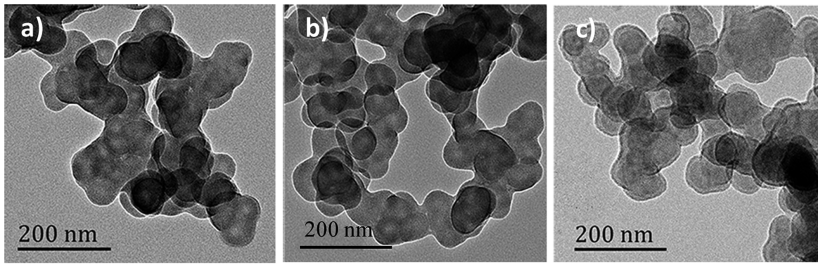

Figure 3. Transmission electron microscope (TEM) images of (A) LP, (B) LD, and (C) LDP. An obvious outer layer (lighter shell/darker core) was found on the surface of LDP. LDP assumes a core−shell structure suggesting that PEG−PLA was coated onto LD.

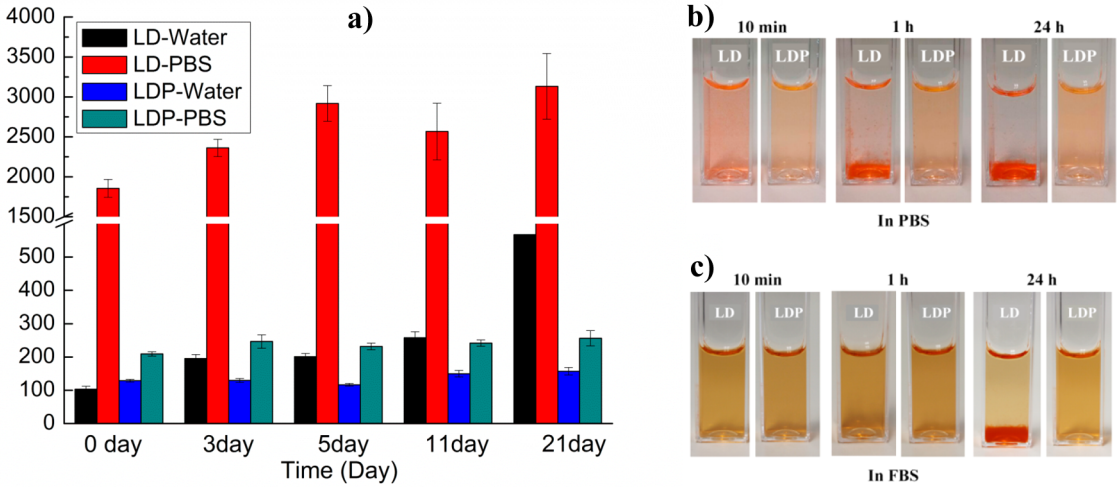

Figure 4. (a) Stability of LD and LDP nanohybrids in water and PBS solution. The dispersed state of LD or LDP in (b) PBS and (c) FBS. Although LD exhibited a nanosize in water, it quickly aggregated into microparticles in PBS.However, LDP can maintain its nanosized state along 21 days, indicating its improved colloidal stability.

surface of the LD nanocomplexes during the mixing process in water/ethanol solution. The hydrophilic PEG moieties that are linked to the PLA will then behave as a protective shell that provides a good steric hindrance, preventing LDP aggregation and ionic interactions between LDP and other molecules (such as FBS proteins). The PEG−PLA coating will thus help maintaining the stability of the whole nanohybrids.[41−47]

Drug Release from DOX-Loaded LP and LDP Nanohybrids. For antitumor therapeutic applications, the encapsulated DOX should be effectively released into the cytoplasm and reach the nucleus to exert its biological activity. To understand the release ability of LDP nanohybrids, we investigated their cumulative release profiles in PBS solution at different pH values (7.4, 6.5, 5.0), as a function of soaking time (Figure 5). The results indicate that DOX was sustainably released from the LDP nanohybrids in PBS solution under all studied pH values for 5 days, compared to the burst release of the free DOX drug (almost all DOX was released in 3 h). On the other hand, the release of DOX from the nanohybrids seemed to be enhanced by decreasing the pH value, revealing that the nanohybrids are pH sensitive. Although the drug release behavior at pH 6.5 (conditions mimicking the extracellular environment of a solid tumor) is very similar to that at pH 7.4, the pH responsive effect is clearly noticeable under acidic conditions that mimic the endolysosomal internal milieu (pH 5.0).[48,49] In this case, the LDP nanohybrids offered

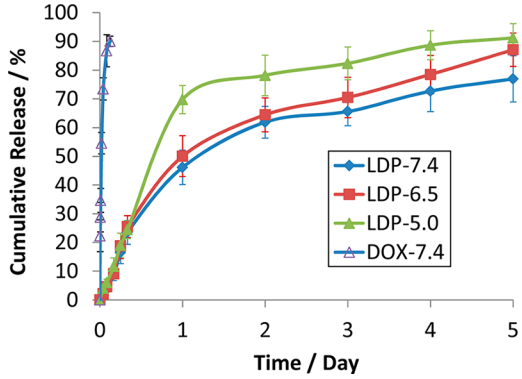

Figure 5. Cumulative release profiles for free DOX and LDP nanohybrids at different pH values (7.4, 6.5, 5.0), in PBS solution, and as a function of soaking time. The LDP nanohybrids had a significantly accelerated DOX release ability under the endolysosomal acidic conditions (pH 5.0).

a significantly accelerated DOX release ability compared to that at physiological pH conditions, especially for early time stages.

It should be noticed that, because free DOX is a weak base with a pK_a of 8.30, it can be easily ionized under acidic conditions, which increases the risk of its trapping in biological acidic compartments like the extracellular space in solid tumors and the endolysosomal cellular compartments.[3,24] The use of nanocarriers can, thus, help to overcome this problem that is

often associated with DOX resistance.[3] Note that, in general, the uptake process of nanoparticles happens in several hours.[50] Therefore, as DOX is carried by the LDP nanohybrids, its trapping can be avoided in the extracellular environment of the solid tumor (pH 6.5).[3] Additionally, the sustained drug release behavior (that does not significantly differ between the pH of 7.4 and 6.5) helps to maintain a high drug loading in the nanohybrids. After cellular internalization, the drug release will be greatly accelerated in the endolysosomal compartments (pH 5.0), possibly counteracting DOX trapping and enhancing its cytotoxicity.[51,52] It has to be noted that although LD nanohybrids also exhibit pH sensitivity in DOX release, its physiological instability will limit their in vivo application (see Figure S1 in the Supporting Information and Figure 2).[38−40]

Cytotoxicity and Cellular Internalization of DOX-Loaded LP and LDP Nanohybrids. The cytotoxicity of the DOX-loaded nanohybrids was quantitatively evaluated using CAL-72 cells (an osteosarcoma cell line) through the resazurin reduction assay (Figure 6). It can be seen that both LD and LDP significantly showed enhanced cytotoxicity toward CAL-72 cells, whereas free DOX alone underwent an expected mild drug resistance.[3] The blank LP and PEG−PLA did not display any cytotoxicity, revealing that the cytotoxic effect was only due to the drug loaded within the nanohybrids. Most importantly, even at very low DOX concentration (0.5 μM), LDP or LD produced an impressively higher cytotoxicity (40 ± 5% or 40 ± 6% of cell viability) than free DOX drug (70 ± 11% of cell viability). The cytotoxicity of the DOX-loaded nanohybrids was also evaluated using NIH 3T3 cells (a noncancerogenic cell line, used as a model of normal cells). As usually happens, the cytotoxicity was higher toward these cells (see Figure S3 in the Supporting Information), but, for in vivo applications, one should expect a higher effect on the tumor site because of the EPR effect.

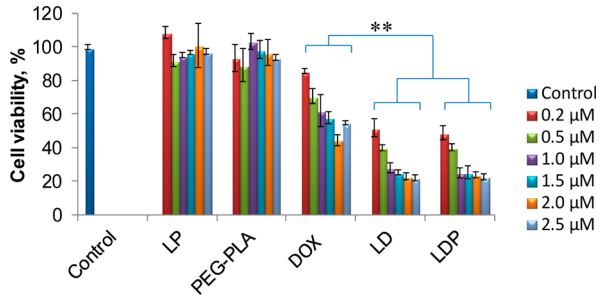

Figure 6. Cell viability/cytotoxicity of free DOX, LD, and LDP nanohybrids (with equivalent DOX concentration) and LP, PEG−PLA (with equivalent weight concentration of the corresponding LDP nanohybrids) after 48 h of cell culture with the CAL-72 cell line (±standard deviation, n = 3, $^{**}p < 0.01$). The LDP and LD nanohybrids presented a significantly higher anticancer cytotoxicity when compared to free DOX.

The optical microscopy was further used to visualize the cell morphology of CAL-72 cells after 48 h culture with the nanoparticles (shown in Figure 7). It can be seen that almost all of the cells cultured with LD and LDP nanohybrids died, while samples treated with free DOX presented a moderate level of cytotoxicity. Although LD exhibited a similar cytotoxicity comparable to LDP, the colloidal instability of the former would be a bottleneck for their further in vivo application because of a limited circulation period. Therefore, the therapeutic efficacy and excellent stability of LDP nanohybrids make them a promising platform for the intracellular delivery of anticancer therapeutic agents.

The drug delivery systems should be effectively taken up by cells and be able to deliver the drug inside them.[53] As DOX is a fluorescent molecule, its internalization by CAL-72 cells can be followed by fluorescence microscopy. Figure 8 shows the bright field and fluorescence microscope images of CAL-72 cells after 48 h in culture with H_2O (control), free DOX (2.5 μM), LD and LDP nanohybrids with an equivalent amount of DOX (2.5 μM) diluted in the cell culture medium. The results show that a higher reddish intensity can be observed inside both cytosol and nucleus (especially in nucleus) after the cells were treated with the LDP nanohybrids for 2 h, compared to free DOX and LD experiments (see Figure 2S in the Supporting Information). This higher DOX accumulation and enhanced anticancer activity may be attributed to the higher cell uptake of the LDP (probably due to their smaller size when compared with LD), as well as to a facilitated DOX release from the endolysosomal compartments to the nucleus.[54] This effect was even more

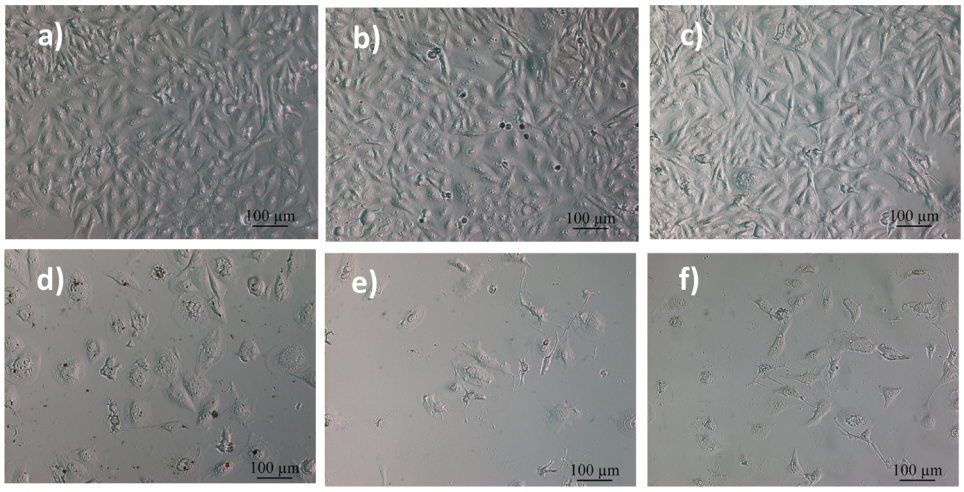

Figure 7. Cell morphology (optical microscopy) of CAL-72 cells after 48 h in culture with (a) control, (b) LP, (c) PEG−PLA, (d) free DOX (2.5 μM), (e) LD, and (f) LDP with an equivalent DOX concentration (2.5 μM). Significant cell death occurred when cells were cultured in the presence of LD and LDP nanohybrids.

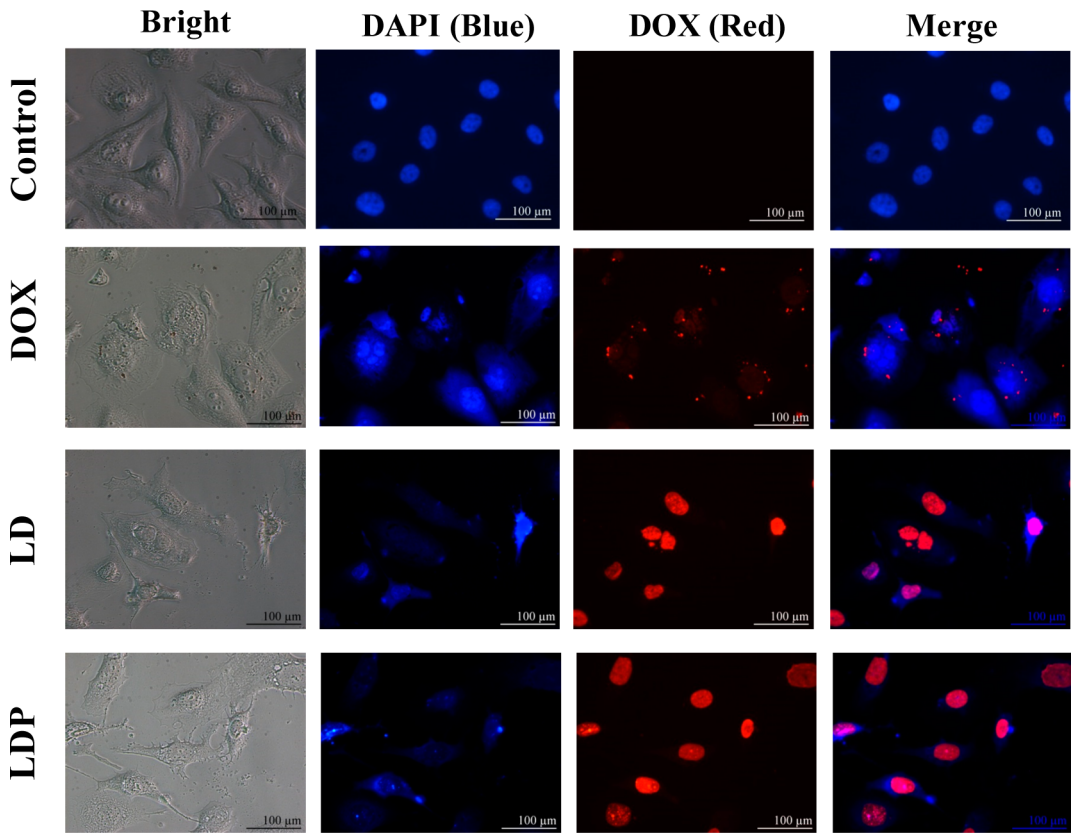

Figure 8. Bright-field and fluorescence microscope images of CAL-72 cells after 48 h culture in the presence of H_2O (control), free DOX (2.5 μM), LD, and LDP nanohybrids with an equivalent amount of DOX (2.5 μM). The cells treated with the LDP nanohybrids presented a higher reddish intensity inside both cytosol and nucleus (especially in the nucleus), indicating the ability of the nanohybrids to enhance DOX accumulation inside cells.

evident after 48 h incubation. After this period, a strong reddish intensity was found inside cells, especially in cell nucleus for CAL-72 cells treated with LD or LDP nanohybrids, whereas only a slight reddish intensity existed in the cytosol for cells treated with free DOX (Figure 8). The above results indicate that the LDP nanohybrids are able to effectively deliver DOX inside cancer cells.

The merits of these nanocarriers, including their biocompatibility and stability, as well as their loading capacity, pH sensitivity in drug release, and improved anticancer cytotoxicity, make them good candidates for delivery of DOX. As a type of smectite clay, the various types of interactions that Laponite can establish with organic molecules, such as hydrophobic interactions, hydrogen bonding, and electrostatic interactions, confer the formed nanohybrids the capability of delivering other cationic or hydrophobic anticancer drugs, beyond doxorubicin.[25,26,55] Although there are other smectite clays with negative-charged surfaces that can be used in the fabrication of nanosystems for drug delivery via a similar method, the synthetic nature of Laponite is an advantage since it minimizes the risk of having impurities compared to natural clays.[55] Furthermore, its special nanodisk structure is an additional advantage among other clays for the development of nanocarriers for anticancer drug delivery.[24] Compared to other nanosystems which have been used for DOX delivery, including PAMAM dendrimers (nondegradable),[10] liposomes (unstable),[11] micelles (unstable),[12] carbon nanotubes (nondegradable),[56] nanogels,[57] the developed LDP nanohybrids have better combined properties, including colloidal stability, biodegradability, and stimuli-responsiveness for therapeutic delivery.

CONCLUSIONS

In summary, we report a simple strategy to develop Laponite/polymer nanohybrids that have good cytocompatibility, sustained pH-responsive release properties, and excellent physiological stability. The hydrophobic block of the amphiphilic PEG–PLA copolymer can act as an anchor to cover the surface of DOX-loaded LP nanodisks, maintaining the core structure, while the hydrophilic PEG part serves as a protective stealth shell to improve the nanohybrid physiological stability. This work gives new insight for the rational design of an optimal platform for the intracellular delivery of therapeutic agents.

ASSOCIATED CONTENT

Supporting Information

Details of drug release profiles of LD in PBS solution at different pH values (7.4, 6.5, 5.0). Bight field and fluorescence microscope images of CAL-72 cells after 2 h culture with the nanohybrids. Cell viability/cytotoxicity of the nanohybrids after 48 h of cell culture with the NIH 3T3 cells (used as model of normal cells). This material is available free of charge via the Internet at http://pubs.acs.org.

AUTHOR INFORMATION

Corresponding Authors

*E-mail: yulinli@uma.pt or yulinli@ecust.edu.cn. Tel.: +351-291705116. Fax: +351-291705149.
*E-mail: lenat@uma.pt

Author Contributions

†G.W. and D.M. equally contributed to this work.

Notes

The authors declare no competing financial interest.

ACKNOWLEDGMENTS

This research was supported by Fundação para a Ciência e a Tecnologia (FCT-IP) with Portuguese Government funds through the CQM Strategic Project PEst-OE/QUI/UI0674/2011-2013, and partially the Project PTDC/CTM-NAN/116788/2010 and the project PTDC/CTM-NAN/112428/2009. FCT-IP is also acknowledged for the Science 2008 Programme (Y.L.). X.S. thanks FCT-IP and Santander Bank for the Invited Chair in Nanotechnology.

REFERENCES

(1) Happell, B.; Scott, D.; Platania-Phung, C. Provision of Preventive Services for Cancer and Infectious Diseases Among Individuals with Serious Mental Illness. *Arch. Psychiat. Nurs.* **2012**, *26*, 192−201.

(2) Tacar, O.; Sriamornsak, P.; Dass, C. R. Doxorubicin: an Update on Anticancer Molecular Action, Toxicity and Novel Drug Delivery Systems. *J. Pharm. Pharmacol.* **2013**, *65*, 157−170.

(3) Yin, Q.; Shen, J.; Zhang, Z.; Yu, H.; Li, Y. Reversal of Multidrug Resistance by Stimuli-Responsive Drug Delivery Systems for Therapy of Tumor. *Adv. Drug Delivery Rev.* **2013**, *65*, 1699−715.

(4) MacKay, J. A.; Chen, M.; McDaniel, J. R.; Liu, W.; Simnick, A. J.; Chilkoti, A. Self-assembling Chimeric Polypeptide−Doxorubicin Conjugate Nanoparticles that Abolish Tumours after a Single Injection. *Nat. Mater.* **2009**, *8*, 993−999.

(5) Yang, J.; Lee, C. H.; Park, J.; Seo, S.; Lim, E. K.; Song, Y. J.; Suh, J. S.; Yoon, H. G.; Huh, Y. M.; Haam, S. Antibody Conjugated Magnetic PLGA Nanoparticles for Diagnosis and Treatment of Breast Cancer. *J. Mater. Chem.* **2007**, *17*, 2695−2699.

(6) Yu, M. K.; Jeong, Y. Y.; Park, J.; Park, S.; Kim, J. W.; Min, J. J.; Kim, K.; Jon, S. Drug-Loaded Superparamagnetic Iron Oxide Nanoparticles for Combined Cancer Imaging and Therapy *in vivo*. *Angew. Chem., Int. Ed.* **2008**, *47*, 5362−5365.

(7) Barraud, L.; Merle, P.; Soma, E.; Lefrançois, L.; Guerret, S.; Chevallier, M.; Dubernet, C.; Couvreur, P.; Trépo, C.; Vitvitski, L. Increase of Doxorubicin Sensitivity by Doxorubicin-Loading into Nanoparticles for Hepatocellular Carcinoma Cells *in vitro* and *in vivo*. *J. Hepatol.* **2005**, *42*, 736−743.

(8) Gonçalves, M.; Figueira, P.; Maciel, D.; Rodrigues, J.; Shi, X.; Tomás, H.; Li, Y. Antitumor Efficacy of Doxorubicin-Loaded Laponite/Alginate Hybrid Hydrogels. *Macromol. Biosci.* **2013**, *14*, 110−120.

(9) Swain, S. M.; Whaley, F. S.; Ewer, M. S. Congestive Heart Failure in Patients Treated with Doxorubicin. *Cancer* **2003**, *97*, 2869−2879.

(10) Lee, C. C.; Gillies, E. R.; Fox, M. E.; Guillaudeu, S. J.; Fréchet, J. M.; Dy, E. E.; Szoka, F. C. A Single Dose of Doxorubicin-Functionalized Bow-Tie Dendrimer Cures Mice Bearing C-26 Colon Carcinomas. *Proc. Natl. Acad. Sci. U.S.A.* **2006**, *103*, 16649−16654.

(11) Batist, G.; Ramakrishnan, G.; Rao, C. S.; Chandrasekharan, A.; Gutheil, J.; Guthrie, T.; Shah, P.; Khojasteh, A.; Nair, M. K.; Hoelzer, K. Reduced Cardiotoxicity and Preserved Antitumor Efficacy of Liposome-Encapsulated Doxorubicin and Cyclophosphamide Compared with Conventional Doxorubicin and Cyclophosphamide in a Randomized, Multicenter Trial of Metastatic Breast Cancer. *J. Clin. Oncol.* **2001**, *19*, 1444−1454.

(12) Yoo, H. S.; Park, T. G. Folate Receptor Targeted Biodegradable Polymeric Doxorubicin Micelles. *J. Controlled Release* **2004**, *96*, 273−283.

(13) Wang, S.; Wu, Y.; Guo, R.; Huang, Y.; Wen, S.; Shen, M.; Wang, J.; Shi, X. Laponite Nanodisks as an Efficient Platform for Doxorubicin Delivery to Cancer Cells. *Langmuir* **2013**, *29*, 5030−5036.

(14) Zhang, X.; Meng, L.; Lu, Q.; Fei, Z.; Dyson, P. J. Targeted Delivery and Controlled Release of Doxorubicin to Cancer Cells Using Modified Single Wall Carbon Nanotubes. *Biomaterials* **2009**, *30*, 6041−6047.

(15) Yu, S. Y.; Hu, J. H.; Pan, X. Y.; Yao, P.; Jiang, M. Stable and pH-Sensitive Nanogels Prepared by Self-Assembly of Chitosan and Ovalbumin. *Langmuir* **2006**, *22*, 2754−2759.

(16) Cheng, R.; Meng, F. H.; Deng, C.; Klok, H. A.; Zhong, Z. Y. Dual and Multi-Stimuli Responsive Polymeric Nanoparticles for Programmed Site-Specific Drug Delivery. *Biomaterials* **2013**, *34*, 3647−3657.

(17) Brannon-Peppas, L.; Blanchette, J. O. Nanoparticle and Targeted Systems for Cancer Therapy. *Adv. Drug Delivery Rev.* **2012**, *64*, 206−212.

(18) Viseras, C.; Cerezo, P.; Sanchez, R.; Salcedo, I.; Aguzzi, C. Current Challenges in Clay Minerals for Drug Delivery. *Appl. .Clay Sci.* **2010**, *48*, 291−295.

(19) Thompson, D. W.; Butterworth, J. T. The Nature of Laponite and Its Aqueous Dispersions. *J. Colloid Interface Sci.* **1992**, *151*, 236−243.

(20) Li, Y.; Santos, J.; Maciel, D.; Tomás, H.; Rodrigues, J. Injectable Hybrid Laponite/Alginate Hydrogels for Sustained Release of Methylene Blue. *J. Controlled Release* **2011**, *152* (Suppl 1), e55−57.

(21) Gaharwar, A. K.; Mihaila, S. M.; Swami, A.; Patel, A.; Sant, S.; Reis, R. L.; Marques, A. P.; Gomes, M. E.; Khademhosseini, A. Bioactive Silicate Nanoplatelets for Osteogenic Differentiation of Human Mesenchymal Stem Cells. *Adv. Mater.* **2013**, *25*, 3329−3336.

(22) Dawson, J. I.; Oreffo, R. O. Clay: New Opportunities for Tissue Regeneration and Biomaterial Design. *Adv. Mater.* **2013**, *25*, 4069−4086.

(23) Okada, A.; Usuki, A. Twenty Years of Polymer-Clay Nanocomposites. *Macromol. Mater. Eng.* **2006**, *291*, 1449−1476.

(24) Goncalves, M.; Figueira, P.; Maciel, D.; Rodrigues, J.; Qu, X.; Liu, C.; Tomás, H.; Li, Y. pH-sensitive Laponite®/Doxorubicin/Alginate Nanohybrids with Improved Anticancer Efficacy. *Acta Biomater.* **2014**, *10*, 300−307.

(25) Jung, H.; Kim, H. M.; Bin Choy, Y.; Hwang, S. J.; Choy, J. H. Laponite-Based Nanohybrid for Enhanced Solubility and Controlled Release of Itraconazole. *Int. J. Pharm.* **2008**, *349*, 283−290.

(26) Takahashi, T.; Yamada, Y.; Kataoka, K.; Nagasaki, Y. Preparation of a Novel PEG-Clay Hybrid as a DDS Material: Dispersion Sability and Sustained Release Profiles. *J. Controlled Release* **2005**, *107*, 408−416.

(27) Fang, J.; Nakamura, H.; Maeda, H. The EPR effect: Unique Features of Tumor Blood Vessels for Drug Delivery, Factors Involved, and Limitations and Augmentation of the Effect. *Adv. Drug Delivery Rev.* **2011**, *63*, 136−151.

(28) Moghimi, S. M.; Davis, S. S. Innovations in Avoiding Particle Clearance from Blood by Kupffer Cells - Cause for Reflection. *Crit. Rev. Ther. Drug Carrier Syst.* **1994**, *11*, 31−59.

(29) Li, Y. H.; Wang, J.; Wientjes, M. G.; Au, J. L. S. Delivery of Nanomedicines to Extracellular and Intracellular Compartments of a Solid Tumor. *Adv. Drug Deliver. Rev.* **2012**, *64*, 29−39.

(30) Delair, T. Colloidal Polyelectrolyte Complexes of Chitosan and Dextran Sulfate Towards Versatile Nanocarriers of Bioactive Molecules. *Eur. J. Pharm. Biopharm.* **2011**, *78*, 10−18.

(31) Douglas, K. L.; Piecirillo, C. A.; Tabrizian, M. Effects of Alginate Inclusion on the Vector Properties of Chitosan-Based Nanoparticles. *J. Controlled Release* **2006**, *115*, 354−361.

(32) Li, Y. L.; Rodrigues, J.; Tomás, H. Injectable and Biodegradable Hydrogels: Gelation, Biodegradation and Biomedical Applications. *Chem. Soc. Rev.* **2012**, *41*, 2193−2221.

(33) Parveen, S.; S, S. K. Evaluation of Cytotoxicity and Mechanism of Apoptosis of Doxorubicin Using Folate-decorated Chitosan Nanoparticles for Targeted Delivery to Retinoblastoma. *Cancer Nanotechnol.* **2010**, *1*, 47−62.
(34) Kayal, S.; Ramanujan, R. V. Doxorubicin Loaded PVA Coated Iron Oxide Nanoparticles for Targeted Drug Delivery. *Mater. Sci. Eng., C* **2010**, *30*, 484−490.
(35) Wang, S. G.; Zheng, F. Y.; Huang, Y. P.; Fang, Y. T.; Shen, M. W.; Zhu, M. F.; Shi, X. Y. Encapsulation of Amoxicillin within Laponite-Doped Poly(lactic-co-glycolic acid) Nanofibers: Preparation, Characterization, and Antibacterial Activity. *ACS Appl. Mater. Interfaces* **2012**, *4*, 6393−6401.
(36) Wang, D. K.; Varanasi, S.; Fredericks, P. M.; Hill, D. J.; Symons, A. L.; Whittaker, A. K.; Rasoul, F. FT-IR Characterization and Hydrolysis of PLA-PEG-PLA Based Copolyester Hydrogels with Short PLA Segments and a Cytocompatibility Study. *J. Polym. Sci., Part A: Polym. Chem.* **2013**, *51*, 5163−5176.
(37) Knop, K.; Hoogenboom, R.; Fischer, D.; Schubert, U. S. Poly(ethylene glycol) in Drug Delivery: Pros and Cons as Well as Potential Alternatives. *Angew. Chem., Int. Ed.* **2010**, *49*, 6288−6308.
(38) Rosenholm, J. M.; Sahlgren, C.; Linden, M. Towards Multifunctional, Targeted Drug Delivery Systems Using Mesoporous Silica Nanoparticles - Opportunities & Challenges. *Nanoscale* **2010**, *2*, 1870−1883.
(39) Bertrand, N.; Leroux, J. C. The journey of a drug-carrier in the body: an anatomo-physiological perspective. *J. Controlled Release* **2012**, *161*, 152−63.
(40) Mangoni, A. A.; Jackson, S. H. D. Age-Related Changes in Pharmacokinetics and Pharmacodynamics: Basic Principles and Practical Applications. *Br. J. Clin. Pharmacol.* **2004**, *57*, 6−14.
(41) Ernsting, M. J.; Tang, W. L.; MacCallum, N. W.; Li, S. D. Preclinical Pharmacokinetic, Biodistribution, and Anti-Cancer Efficacy Studies of a Docetaxel-Carboxymethylcellulose Nanoparticle in Mouse Models. *Biomaterials* **2012**, *33*, 1445−1454.
(42) Zhang, X. D.; Wu, D.; Shen, X.; Chen, J.; Sun, Y. M.; Liu, P. X.; Liang, X. J. Size-Dependent Radiosensitization of PEG-Coated Gold Nanoparticles for Cancer Radiation Therapy. *Biomaterials* **2012**, *33*, 6408−19.
(43) Vonarbourg, A.; Passirani, C.; Saulnier, P.; Simard, P.; Leroux, J. C.; Benoit, J. P. Evaluation of Pegylated Lipid Nanocapsules Versus Complement System Activation and Macrophage Uptake. *J. Biomed. Mater. Res., Part A* **2006**, *78A*, 620−628.
(44) Hamad, I.; Al-Hanbali, O.; Hunter, A. C.; Rutt, K. J.; Andresen, T. L.; Moghimi, S. M. Distinct Polymer Architecture Mediates Switching of Complement Activation Pathways at the Nanosphere-Serum Interface: Implications for Stealth Nanoparticle Engineering. *ACS Nano* **2010**, *4*, 6629−6638.
(45) Cho, H. J.; Yoon, I. S.; Yoon, H. Y.; Koo, H.; Jin, Y. J.; Ko, S. H.; Shim, J. S.; Kim, K.; Kwon, I. C.; Kim, D. D. Polyethylene Glycol-Conjugated Hyaluronic Acid-Ceramide Self-Assembled Nanoparticles for Targeted Delivery of Doxorubicin. *Biomaterials* **2012**, *33*, 1190−1200.
(46) Naeye, B.; Raemdonck, K.; Demeester, J.; De Smedt, S. C. Interactions of siRNA Loaded Dextran Nanogel with Blood Cells. *J. Controlled Release* **2010**, *148*, E90−E91.
(47) Bhadra, D.; Bhadra, S.; Jain, S.; Jain, N. K. A PEGylated Dendritic Nanoparticulate Carrier of Fluorouracil. *Int. J. Pharm.* **2003**, *257*, 111−124.
(48) Mahoney, B. P.; Raghunand, N.; Baggett, B.; Gillies, R. J. Tumor Acidity, Ion Trapping and Chemotherapeutics I. Acid pH Affects the Distribution of Chemotherapeutic Agents in vitro. *Biochem. Pharmacol.* **2003**, *66*, 1207−1218.
(49) Wojtkowiak, J. W.; Verduzco, D.; Schramm, K. J.; Gillies, R. J. Drug Resistance and Cellular Adaptation to Tumor Acidic pH Microenvironment. *Mol. Pharm.* **2011**, *8*, 2032−2038.
(50) Maciel, D.; Figueira, P.; Xiao, S. L.; Hu, D. M.; Shi, X. Y.; Rodrigues, J.; Tomás, H.; Li, Y. L. Redox-Responsive Alginate Nanogels with Enhanced Anticancer Cytotoxicity. *Biomacromolecules* **2013**, *14*, 3140−3146.
(51) Oishi, M.; Sumitani, S.; Nagasaki, Y. On-off Regulation of F-19 Magnetic Resonance Signals Based on pH-Sensitive PEGylated Nanogels for Potential Tumor-Specific Smart F-19 MRI Probes. *Bioconjugate Chem.* **2007**, *18*, 1379−1382.
(52) Yang, J.; Chen, H. T.; Vlahov, I. R.; Cheng, J. X.; Low, P. S. Characterization of the pH of Folate Receptor-Containing Endosomes and the Rate of Hydrolysis of Internalized Acid-Labile Folate-Drug Conjugates. *J. Pharmacol. Exp. Ther.* **2007**, *321*, 462−468.
(53) Santos, J. L.; Oliveira, H.; Pandita, D.; Rodrigues, J.; Pego, A. P.; Granja, P. L.; Tomás, H. Functionalization of Poly(amidoamine) Dendrimers with Hydrophobic Chains for Improved Gene Delivery in Mesenchymal Stem Cells. *J. Controlled Release* **2010**, *144*, 55−64.
(54) Harush-Frenkel, O.; Debotton, N.; Benita, S.; Altschuler, Y. Targeting of Nanoparticles to the Clathrin-Mediated Endocytic Pathway. *Biochem. Biophys. Res. Commun.* **2007**, *353*, 26−32.
(55) Dawson, J. I.; Oreffo, R. O. C. Clay: New Opportunities for Tissue Regeneration and Biomaterial Design. *Adv. Mater.* **2013**, *25*, 4069−4086.
(56) Zhang, X. K.; Meng, L. J.; Lu, Q. H.; Fei, Z. F.; Dyson, P. J. Targeted Delivery and Controlled Release of Doxorubicin to Cancer Cells Using Modified Single Wall Carbon Nanotubes. *Biomaterials* **2009**, *30*, 6041−6047.
(57) Goncalves, M.; Figueira, P.; Maciel, D.; Capelo, D.; Xiao, S.; Sun, W.; Rodrigues, J.; Shi, X.; Tomás, H.; Li, Y. Dendrimer-Assisted Formation of Fluorescent Nanogels for Drug Delivery and Intracellular Imaging. *Biomacromolecules* **2014**, *15*, 492−499.